Imbibition of Solids in Nanopillar Arrays

Philippe Gaillard,[1] Yukio Saito,[2] and Olivier Pierre-Louis[1]

[1]*Laboratoire de Physique de la Matière Condensée et Nanostructures, 43 Boulevard du 11 novembre 1918, Université Claude Bernard Lyon 1, F 69622 Villeurbanne, France*

[2]*Department of Physics, Keio University, 3-14-1 Hiyoshi, Kohoku-ku, Yokohama, Japan*

(Received 23 February 2011; published 10 May 2011)

The imbibition of a solid island on a substrate with a square array of pillars is studied by means of kinetic Monte Carlo simulations. Imbibition is found to occur via an intermediate state where an island sits on the film. Two dynamical regimes are identified depending on the geometry of the substrate: a stochastic regime, where the dynamics are controlled by the nucleation-limited motion of the imbibition front across the array of pillars, and a deterministic regime limited by the diffusion of atoms on top of the imbibition film.

DOI: 10.1103/PhysRevLett.106.195501 PACS numbers: 81.10.Aj, 68.55.−a

Many processes are now known to produce nanoscale solid islands and films, such as epitaxial growth [1–3], cluster deposition [4], dewetting under annealing [5,6], or under pulsed lasers [7]. During these formation processes, the shape of islands and films is usually not well controlled and results from a delicate interplay between energetics and kinetics. In addition, the island shape usually irredeemably relaxes towards the unique equilibrium shape fixed by the orientation-dependent surface free energy.

However, some control in the island shape could be obtained in the presence of elastic epitaxial strain, leading, for example, to nanowires [8]. Recently, it was proposed that, in addition to its well established role in the control of island positioning [9–11], substrate nanopatterning may also offer control over the island shape [12], and maintain islands in metastable states. Following this line of investigation, shape multistability was found for island relaxation on nanogrooves [12], and island growth on nanopillars in experiments [13] and in theory [14]. In this Letter, we propose an additional scenario, henceforth denoted as "solid imbibition," by which the islands may penetrate the nanopatterns and form a film. This phenomenon shares similarities with the imbibition of liquids [15] in micropatterns. Since it allows one to control the shape of the film, liquid imbibition dynamics have received recent attention [16–18]. Here, we hope to provide some hints towards similar control of the film morphology for solids. Based on kinetic Monte Carlo (KMC) simulations, we find that imbibition occurs via an intermediate, transient state where an island sits on the top of the film. In addition, we find two possible dynamic regimes: (i) a stochastic nucleation-limited regime, and (ii) a deterministic diffusion-limited regime. Simple analytical models allow us to analyze the results. Finally, the relevance of our results for experiments is discussed.

Our work also provides some hints towards a better microscopic understanding of the growth of reconstruction domains around decaying islands [19], which involves similar redistribution of mass at the nanoscale as imbibition. In addition, imbibition is a key concept towards the modeling of the growth of thin films on nanoporous substrates which may—as for Ge on nanoporous Si [20], or may not—as for GaN on nanoporous Si [21,22], penetrate the pores.

We use a 3D KMC model on a cubic lattice [12,14], where each site may be unoccupied, occupied by an adsorbate atom, or occupied by a substrate atom. The substrate is assumed to be frozen. The cohesion of the adsorbate is maintained by bonds of energy J_1 to nearest neighbors (NN), and J_2 to next-nearest-neighbor (NNN) adatoms. The ratio $\zeta = J_2/J_1$ controls the equilibrium shape of a freestanding adsorbate crystal. When $\zeta = 0$, the equilibrium shape is a cube with (100) facets only. When $\zeta > 0$, (110) and (111) facets appear [12]. Adatoms also interact with substrate atoms up to the second neighbor, with bond energies J_{s1} and J_{s2}. We arbitrarily set $J_{s2}/J_{s1} = J_2/J_1 = \zeta$. The parameter $\chi = J_{s1}/J_1$ defines the wettability of the adsorbate, and plays a role similar to the contact angle for isotropic liquids [23]. On a flat substrate, the island equilibrium shape for a given value of χ is obtained by a truncation of the freestanding equilibrium shape [12]. When $\chi \geq 1$, the adsorbate completely wets the substrate and spreads over a flat substrate. In contrast, when $\chi \to 0$, the adsorbate island shape tends to the untruncated freestanding equilibrium shape, and minimizes its contact area with the substrate.

The island shape relaxes via surface diffusion by allowing jumps of adsorbate atoms to empty surface sites that have at least one NN or NNN bond to another adsorbate atom [24]. For an adatom with n_i neighbors of type $i = 1, 2, s1, s2$ before the jump, the transition frequency is given as $\nu = \nu_0 e^{-\sum_i n_i J_i/T}$. Here, ν_0 is an attempt frequency, and T is the temperature (in units with $k_B = 1$). We use a temperature $T/J_1 = 0.5$, which is high enough to promote shape relaxation, but low enough to keep a faceted island shape.

We use a patterned substrate consisting of a square array of pillars, of period ℓ_x in both x and y directions. Pillars have a height h, and a square cross section of width ℓ_p. Two dimensionless parameters characterize the pattern

geometry: $\phi = \ell_p^2/\ell_x^2$, and $\rho = 4h/\ell_p$. The simulation box is periodic along x and y. We use a square box of size $L_x \times L_x$, and the system height L_z is chosen to be high enough to accommodate the highest islands.

We here present the result of simulations with $\zeta = 0.2$, $\chi = 0.8$, $h = 3$, and $\ell_x = 6$, with different values of ℓ_p. When varying the different parameters (e.g., $\chi = 0.9$, or $h = 4$ or 5, etc.), we obtained qualitatively similar behaviors, and we therefore focus on the restricted set of parameters given above.

We start with a cubic-shaped island, which is in the so-called Wenzel state [25] [depicted at the top of Fig. 1(a)]. The length of the sides of the island is 20, so that the total number of atoms is around 8000. During shape relaxation, three states are observed, as shown in Fig. 1(a): the Wenzel state (W), the island and film state (IF), and the film state (F). The island initially spreads in the W state, then the imbibition film starts to spread faster than the island leading to the IF state. For $\ell_p \geq 2$ we have always obtained the F state as the final state. However, for $\ell_p = 1$, the dynamics drastically slow down, so that we cannot obtain a F state in KMC simulations.

Let us first determine the conditions in which an imbibition film can be formed. Assuming that A is the total substrate area (including the sides of the pillars), and $A_\perp$ is the projected surface area (excluding the sides of the pillars), the film will form when

$$(\gamma_{AS} - \gamma_{SV})(A - \phi A_\perp) + A_\perp(1 - \phi)\gamma_{AV} < 0, \qquad (1)$$

where γ_{AS}, γ_{SV}, and γ_{AV}, respectively, account for the free energies of the adsorbate-substrate (AS) interface, the substrate-vacuum (SV) surface, and the adsorbate-vacuum (AV) surface. The first term in Eq. (1) accounts for the change of the bottom substrate surface and of the pillar side surfaces from SV to AS, and the second term accounts for the formation of the free AV surface of the film. Approximating the (100) facet free energy by its energy [12], one has $1 - 2\chi = (\gamma_{AS} - \gamma_{SV})/\gamma_{AV}$, and from Eq. (1) the formation of an imbibition film is energetically favorable when $\chi > \chi_c$, with

$$\chi_c = \frac{1}{2}\left(1 + \frac{1 - \phi}{r_A - \phi}\right), \qquad (2)$$

where $r_A = A/A_\perp = 1 + \rho\phi$. A similar criterion, relying on the same energy balance analysis, has been derived in the literature for the imbibition of liquids [15]. However, note that criterion (2) for solids is limited to the case of interest for our KMC simulations, where all surfaces and interfaces exhibit the (100) orientation. Using the KMC simulation parameters given above, we find that imbibition at $\chi = 0.8$ should be observed for $\ell_p > 1.82\ldots$. This is in agreement with the simulations, where imbibition was not observed for $\ell_p = 1$, but was observed for $\ell_p \geq 2$.

We now analyze the observed sequence of configurations W, IF, and F. To simplify the analysis, we assume that the island and the film exhibit (100) facets only (a limit which corresponds to $\zeta \to 0$). We also assume that the island on top of the film has relaxed to its equilibrium aspect ratio, so that $h_I/L_I = \phi(1 - \chi)$, where h_I and L_I are the height and the width of the island [Fig. 1(i)].

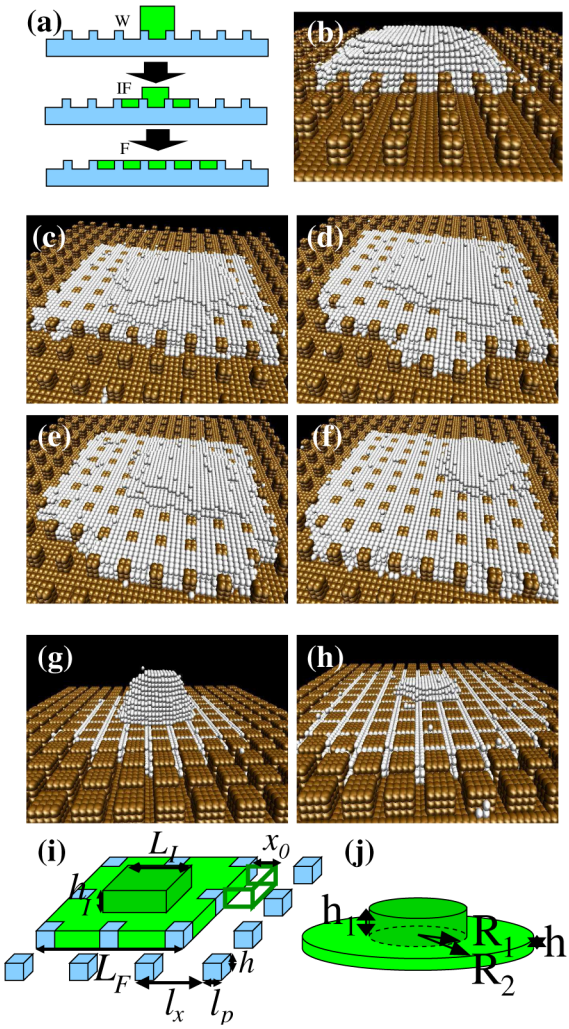

FIG. 1 (color online). KMC simulation results. (a) Sequence of states observed during imbibition dynamics: W, IF, and F. (b)–(f) Regime I for $\ell_p = 2$: (b) initial spreading in the W state, and (d)–(f) IF state. The motion of the imbibition front takes place via a nucleation (d), and zipping (e) mechanism. (g)–(h) Regime II for $l_p = 4$: the film is isotropic (circular), and the film edge motion is not pinned by the pillars. (i) Schematics for regime I. (j) Schematics for regime II.

In a quasistatic picture, the domain of existence of the IF state can be obtained from the geometrical statement that $L_F > L_I > 0$, where L_F is the lateral extent of the film. Considering a fixed total adsorbate volume V, with a film spreading on $n \times n$ pillars, this relation imposes that the IF state exists for $V_{W|IF} > V > V_{IF|F}$, with

$$V_{IF|F} = hL_F^2 - n^2\ell_p^2 h. \qquad (3)$$

$$V_{W|IF} = V_{IF|F} + \phi(1 - \chi)L_F^3. \qquad (4)$$

For the smallest film covering $n \times n$ pillars, as in Fig. 1(a), one has $L_F = (n - 1)\ell_x + \ell_p$. Since n has a clearer

geometrical interpretation, we choose to use n rather than L_F as a control variable in the following. The expected trajectory of the island at fixed V in the (V,n) plane, shown in Fig. 2(a), is in agreement with KMC simulations.

We now discuss the dynamics in more detail. Two regimes, shown in Fig. 1, are observed in KMC simulations. For small values of ℓ_p (large gap $\tilde{\ell}_p \equiv \ell_x - \ell_p$), the film exhibits a square shape, and the island on top of the film is very flat. Hereafter, this regime will be denoted as regime I. For large values of ℓ_p (small gap $\tilde{\ell}_p \equiv \ell_x - \ell_p$), a different regime is observed. The film looks isotropic (its edge is almost circular), and the island exhibits a rough isotropic shape. This second regime will be referred to as regime II. An important difference between the two regimes can be observed: different realizations of the dynamics (with the same initial conditions but different random number generations) lead to the same macroscopic evolution in regime II in Fig. 2(c), while they lead to different ones in regime I in Fig. 2(b). Large fluctuations in regime I suggest that the dynamics are controlled by a stochastic process.

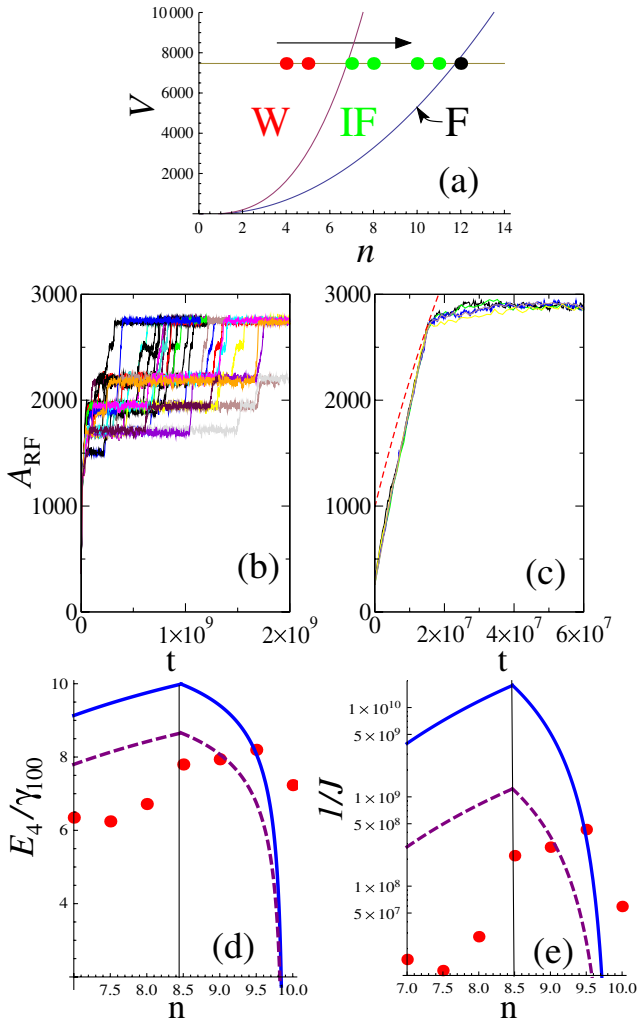

FIG. 2 (color online). Comparison of models with KMC simulations. (a) Island evolution for a fixed volume V, as a function of the number $n \times n$ of substrate pillars covered. The lines are obtained from Eqs. (4) and (3). The dots are approximate points obtained from KMC simulations. (b),(c) Area of contact between the film and the substrate excluding pillars A_{RF} [equal to $(1-\phi)$ times the total film area] as a function of time in (b) regime I with $\ell_p = 2$, and (c) regime II with $\ell_p = 4$. The dashed red line in regime II is the model equation (9). The only fitting parameter is the final collapse time. (d) Nucleation barrier E_4, and (e) waiting time $\mathcal{J}^{-1}$ fort regime I, with $\ell_p = 2$. Solid lines represent model equations (5) and (6), and dots correspond to KMC simulations. Dashed lines include corrections accounting for the (110) facet in the nucleus.

Let us first discuss regime I. Each step in the evolution of the area in Fig. 2(b) corresponds to a forward motion of the film edge from one row to the next one, and follows the same sequence of events: (i) a small localized perturbation of the film edge, forming a "nucleus," reaches neighboring pillars, (ii) a zipping process starts from the nucleus and allows the whole edge to reach the neighboring row of pillars. Since the waiting time before the appearance of the nucleus is much longer than the zipping time, the front motion is controlled by this first nucleation event. We consider a nucleus between four pillar corners, with a length x_0, as shown in Fig. 1(i). (Other configurations have been considered. They lead to higher nucleation barriers, and are therefore irrelevant). Within the approximation that the nucleus volume is much smaller than the island volume, the nucleation barrier E_4 corresponds to the maximum value of $x_0 = \tilde{\ell}_p \equiv \ell_x - \ell_p$:

$$\frac{E_4}{\gamma_{100}} = 2\tilde{\ell}_p\left[\tilde{\ell}_p(1-\chi) + h - \frac{2h\tilde{\ell}_p}{L_*}\right], \tag{5}$$

where $L_* = L_F$ in W state, and $L_* = L_I$ in IF state.

In order to relate the nucleation barrier to a nucleation rate $\mathcal{J}$, we use standard nucleation theory, leading to

$$\mathcal{J} = 4(n-1)\tilde{\ell}_p D c_{eq} e^{-E_4/k_B T}, \tag{6}$$

where c_{eq} and D are the equilibrium concentration and the diffusion constant on top of the film. Since $\chi = 0.8$ is close to 1, there is no significant difference in the hopping rate between diffusion on the film and diffusion on top of the pillars, so we shall approximate D by the diffusion constant along a (100) adsorbate surface, leading to $D \approx a^2 \nu_0 e^{-J_1(1+4\zeta)/T}$. In addition, one finds that $c_{eq} = e^{-2J_1(1+\zeta)/T}$ from the detailed balance between a mobile atom and a kink site.

In Fig. 2(e), we have measured the average waiting times before the formation of a new row in KMC over 30 simulations, for the $\ell_p = 2$ case. Here n is defined as $n = (n_x + n_y)/2$, where n_x and n_y are the number of pillars covered by the film in the x and y directions. From these waiting times $\sim 1/\mathcal{J}$, we may extract an effective nucleation barrier from KMC, using Eq. (6). The result is plotted in Fig. 2(d). We have obtained a reasonably good approximation for the nucleation barrier [a model accounting for

(110) facets gives slightly better agreement, as shown in Figs. 2(d) and 2(e)]. However, due to the exponential dependence of $\mathcal{J}$ in E_4, the small inaccuracy of E_4 (20%) leads to a large inaccuracy on $\mathcal{J}$.

In order to model regime II, we have derived the film area evolution from a simplified axisymmetric model, shown in Fig. 1(j), where atoms diffuse between the central island and the film edge. We assume once again that the top island instantaneously relaxes to its equilibrium shape. The local chemical potentials in the vicinity of the top island and film edges read

$$\mu_1 = \frac{2\Omega\gamma_{\mathrm{AV}}}{R_1}; \qquad \mu_2 = \frac{2\Omega\gamma_{\mathrm{AV}}(\chi_c - \chi)}{h(2\chi_c - 1)}. \tag{7}$$

We assume local equilibrium between the film edge and the island edge, so that $c|_{r=\mathrm{R}_i} \approx c_{eq}(1 + \mu_i/k_{\mathrm{B}}T)$, with $i = 1, 2$. We also assume that the concentration c of mobile atoms on top of the film obeys a quasistatic diffusion equation $D\nabla^2 c = 0$. Finally, mass conservation imposes

$$\partial_t V_i = (-1)^{i+1} 2\pi\Omega R_i D \partial_r c|_{r=\mathrm{R}_i}, \tag{8}$$

where $i = 1, 2$, and V_1 and V_2 are the volume of the island and the film, respectively.

We consider the intermediate regime where the island volume is smaller than the film volume $V_1 = \pi R_1^2 h_1 \ll V$, but the island volume is not too small, so that $|\mu_2| \gg |\mu_1|$. The latter condition will be fulfilled when h/R_1 is small or when $\phi \to 1$. We then obtain the evolution of the film area $A_2 = \pi R_2^2$ as

$$\mathcal{A}_2\left(1 - \ln\left[\frac{\upsilon^{-3/2}\mathcal{A}_2}{\pi 2\phi(1-\chi)}\right]\right) = \frac{3\pi\mu_2\Omega D C_{eq}(t_0 - t)}{2k_B T}, \tag{9}$$

where $\mathcal{A}_2 = V - A_2 h(1 - \phi)$, $\upsilon = V/[(1 - \phi)\pi h]$, and t_0 is the collapse time when the top island disappears. Hence, A_2 is linear in time up to logarithmic corrections. Using Eq. (9), we obtain good agreement with no fitting parameter as compared to KMC simulations with $h = 3$ and $\ell_p = 4$, as shown by the dashed line in Fig. 2(c). These results confirm that dynamics in regime II are indeed limited by adatom diffusion on the film.

Finally, we discuss the major constraints for observing imbibition in experiments. Since $\chi_c > 0.5$, the first constraint is to consider systems with large values of $\chi > 0.5$. Such values are, for example, observed for Si/SiO_2, with $\chi \approx 0.65$ [26], or $Cu/Ti/SiO_2$ [27] with $\chi = 0.8$. The second constraint is the smallness of the gap between pillars, which is required in order to keep E_4 small enough for the nucleation of new rows to occur in observable time. This leads to gaps smaller than 10 nm [28]. Such nanostructures can be obtained either by spontaneous structure formation during growth [3], and molecular films [29], or from the focused ion beam lithography [30].

In summary, solid imbibition follows a sequence of three states: Wenzel, island plus film, and film. We have observed two types of imbibition dynamics: (I) a stochastic nucleation-limited regime with an anisotropic film shape, and (II) a deterministic diffusion-limited regime with an isotropic film shape. A quantitative discussion of the results allows us to claim that imbibition should be observable in systems with large wettability ($\chi > 0.5$), and with nanoscale patterns.

[1] A. Pimpinelli and J. Villain, *Physics of Crystal Growth* (Cambridge University Press, Cambridge, U.K., 1998).
[2] T. Michely and J. Krug, *Islands, Mounds, and Atoms* (Springer, New York, 2004).
[3] C. Misbah, O. Pierre-Louis, and Y. Saito, Rev. Mod. Phys. **82**, 981 (2010).
[4] P. Jensen, Rev. Mod. Phys. **71**, 1695 (1999).
[5] B. Yang *et al.*, Phys. Rev. B **72**, 235413 (2005).
[6] O. Pierre-Louis, A. Chame, and Y. Saito, Phys. Rev. Lett. **103**, 195501 (2009).
[7] H.-J. Ernst, F. Charra, and L. Douillard, Science **279**, 679 (1998).
[8] J. Tersoff and R. M. Tromp, Phys. Rev. Lett. **70**, 2782 (1993).
[9] G. Katsaros *et al.*, Phys. Rev. Lett. **101**, 096103 (2008).
[10] H. Hu, H. J. Gao, and F. Liu, Phys. Rev. Lett. **101**, 216102 (2008).
[11] W. Ling *et al.*, Surf. Sci. Lett. **570**, L297 (2004).
[12] O. Pierre-Louis and Y. Saito, Europhys. Lett. **86**, 46004 (2009).
[13] S. D. Hersee *et al.*, J. Appl. Phys. **97**, 124308 (2005).
[14] K. Takano, Y. Saito, and O. Pierre-Louis, Phys. Rev. B **82**, 075410 (2010).
[15] J. J. Bico *et al.*, Europhys. Lett. **55**, 214 (2001).
[16] L. Courbin *et al.*, Nature Mater. **6**, 661 (2007).
[17] T. Cubaud and M. Fermigier, Europhys. Lett. **55**, 239 (2001).
[18] M. L. Blow, H. Kusumaatmaja, and J. M. Yeomans, J. Phys. Condens. Matter **21**, 464125 (2009).
[19] K. R. Roos *et al.*, Phys. Rev. Lett. **100**, 016103 (2008).
[20] D. Buttard *et al.*, J. Cryst. Growth **183**, 294 (1998).
[21] L. Macht *et al.*, Appl. Phys. Lett. **87**, 131904 (2005).
[22] K. Zang *et al.*, Appl. Phys. Lett. **88**, 141925 (2006).
[23] Using the (100) facet as the reference energy, one may draw a relation between χ and the contact angle θ as $\cos\theta = 2\chi - 1$.
[24] This procedure does not forbid the desorption of dimers from the island. However, this undesirable effect is negligibly small at our typical working temperatures.
[25] R. N. Wenzel, Ind. Eng. Chem. **28**, 988 (1936).
[26] D. Danielson *et al.*, J. Appl. Phys. **100**, 083507 (2006).
[27] M. Hu *et al.*, J. Appl. Phys. **94**, 3492 (2003).
[28] The dominant contribution to E_4 is the term $2\gamma_{100}\tilde{\ell}_p h$. If h is nanometrically small, the edge of the nucleus can be considered as being a bunch of n_h atomic steps, and $\gamma_{100} h = \gamma_s n_h$, where γ_s is the step free energy. Typically, $\gamma_s \sim 0.1$ eV.Å^{-1}, $k_{\mathrm{B}}T \sim 0.1$ eV. For nucleation to be observable, we expect $E_4/k_{\mathrm{B}}T < 30$, which indicates that h, and $\tilde{\ell}_p$ should be not larger than some nanometers.
[29] Z. Cheng *et al.*, Nano Lett. **10**, 3700 (2010).
[30] C. W. Hagen and P. Kruit, J. Vac. Sci. Technol. B **27**, 2654 (2009).